Epitaxial Growth of SiO_2 Produced in Silicon by Oxygen Ion Implantation

V. V. Afanas'ev and A. Stesmans
Department of Physics, University of Leuven, Celestijnenlaan 200D, B-3001 Leuven, Belgium

M. E. Twigg
Electronic Technology Division, Naval Research Laboratory, Washington, DC 20375
(Received 14 May 1996)

Oxide layers produced by implantation of (001) silicon with oxygen were found to contain a crystalline phase in registry with the Si substrate. The crystals resemble the coesite phase of SiO_2 with the *b* axis oriented along a [001] Si substrate direction. Formation of oxide crystals requires confinement of the oxide layer between two silicon layers, indicating the necessity of high pressure for epitaxial growth. [S0031-9007(96)01648-1]

PACS numbers: 61.16.Ch, 61.72.Hh, 68.55.–a

SiO_2 layers formed by silicon oxidation are generally considered to be amorphous (see, e.g., Refs. [1–5], and references therein). Formation of a crystalline epitaxial oxide (tridymite) layer has been suggested, but the crystallinity is already broken within the first elemental unit [6]. Large volume expansion (~126%) associated with incorporation of Si atoms into the oxide and the nonmatching of elemental units of silicon and SiO_2 polymorphs seem to obstruct the epitaxial oxide growth. However, crystalline-shaped inclusions are well known to be formed during oxygen precipitation in silicon [7–9]. Microdiffraction analysis has revealed the presence of a crystalline oxygen-containing phase close to coesite in the precipitates formed under conditions of high oxygen oversaturation of Si and low impurity concentration [10]. These observations refer to the possibility of epitaxiality between Si and SiO_2 under certain conditions. We will show that crystalline oxide, probably in the form of coesite, can be produced by annealing oxygen implanted silicon. The epitaxial formation of the oxide crystallites on a Si(001) surface requires both a high concentration of oxygen and confinement of the oxide by a Si overlayer.

The samples were prepared by implantation of oxygen ions in one or multiple steps [energy $E = 120-210$ keV, dose $D = (0.4-10) \times 10^{18}$ cm^{-2}] into (001) Si wafers. After implantation the samples were annealed in Ar + 0.5% O_2 at 1350 °C for 5 h to obtain a continuous oxide layer of thickness 72–450 nm buried under a top *c*-Si layer 135–320 nm thick. More details can be found in Refs. [11,12]. In a first Si etching step, the top Si layer of the $Si/SiO_2/Si$ structures was removed using a selective wet Si etch. Subsequently, the oxide layer was etched in buffered HF (a highly selective SiO_2 etch); the treatment was stopped when the surface became nonwetting, an indication of silicon coverage. It was found, however, that not all of the oxide disappeared. After removing the outer SiO_2 part, some remained, protectively screened by some remaining Si. Then, to further reveal the surface, the samples were shortly resubmitted to a hot aqueous KOH solution sufficient to remove 40–60 nm of Si. This, indeed, left the surface wetted again, indicative of exposed oxide. Sample surfaces were examined by atomic force microscopy (AFM) operating in a constant force mode (Burleigh ARIS-3500) and transmission electron microscopy (TEM). This was complemented by electron spin resonance (ESR) spectroscopy after bombarding the exposed surface for about 10 min by Ar 400-eV ions. When applied to amorphous (*a*) SiO_2, this treatment very efficiently generates a high local density ($>10^{18}$ cm^{-3}) of E'_γ defects in a surface layer of ~10 nm thick, as outlined previously [13]. The details of the bombardment procedure and ESR measurements have been published elsewhere [13].

The broad scan AFM image of a sample implanted with 1.8×10^{18} O^+/cm^2 at 200 keV after the first oxide etch is shown in Fig. 1. The surface exhibits a two-level structure formed by the Si substrate and tablelike features ~100 nm high. The top view image (not shown) reveals rectangular- or polygonal-shaped features of 100–200 nm wide with the sides oriented along [110], [$\bar{1}$10], and [010]

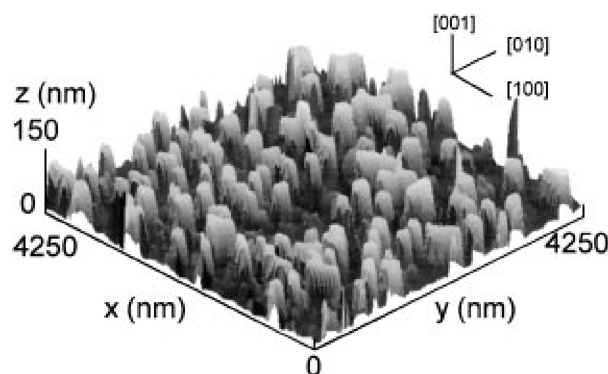

FIG. 1. Three-dimensional AFM image of the sample surface after HF etching to the nonwetting state. The sample was prepared by implanting oxygen (1.8×10^{18} O^+/cm^{-2}, $E =$ 200 keV) in Si(100), followed by a high-temperature anneal at 1350 °C for 5 h.

 0031-9007/96/77(20)/4206(4)$10.00 © 1996 The American Physical Society

directions of the Si substrate. Such Si platelet inclusions in buried oxides formed by oxygen ion implantation in Si have been observed previously by electron microscopy [14,15]. Upon the second short KOH dip, these Si platelets disappear and sharp pyramids appear. This is illustrated in Fig. 2 by the three-dimensional (a) and top (b) views. The sides of the base are oriented along ⟨110⟩ Si directions, with the top pyramid average angle determined as $46° \pm 1°$. The pyramids can be dissolved in HF, suggesting their oxide nature; however, their etch rate was found to be considerably less than that of amorphous SiO_2 (a-SiO_2), which may be indicative of either oxide densification or silicon enrichment. After a prolonged HF etch the silicon surface is hilly with a peak-to-peak height of 10–15 nm, but does not show any distinct crystalline features.

In order to gain insight into the nature of the pyramidal features, the samples were bombarded with Ar ions and the created dangling-bond defects were analyzed by ESR. Silicon dangling bonds are highly sensitive to their surroundings: for example, with three Si atoms in the backbonds, the well-known P_b center is formed; with three oxygen atoms, the E' defect is obtained, both defects being well characterized by their specific g tensor [16]. So if the dangling bonds are produced within a single crystal, the ESR signal will be anisotropic with respect to the direction of the magnetic field **B**. When produced within an amorphous matrix, however, the ESR anisotropy will disappear, the line shape showing a characteristic powder pattern. ESR spectra from a sample with exposed pyramids for two orientations of **B** are compared in Fig. 3 with the spectrum observed on an identically ion-bombarded dry a-SiO_2 layer thermally grown on (001) Si. A signal at $g = 2.0006$, the E'_γ center [16], is observed in both cases, thus proving the Si-oxide nature of the pyramids. A first striking observation, however, is that the characteristic two-peak powder pattern observed in thermal a-SiO_2 (C) is much suppressed in the spectra of the pyramid-covered surfaces; the signal now exhibits some anisotropy, indicating that the E' centers are incorporated into a crystalline rather than an amorphous SiO_2 network. A second important finding is that the generated E'_γ density in the pyramid surface is much less than in a-SiO_2, even when taking into account that the pyramid coverage is only partial (~10%). It refers to the much reduced efficiency of defect production in crystalline quartz [17] as compared to vitreous silica [18], in line with the first observation.

The size of the oxide crystallites is sensitive to the O^+ implantation parameters: The height of the pyramids increases up to 200 nm if the ions are implanted along a Si channeling direction, but decreases down to 40 nm for off-channeling position. It seems to be related to the fact that the projected range of O^+ ions is larger in the channeling geometry [19]. A broader distribution of implanted oxygen ions results, and the size of the crystallites may

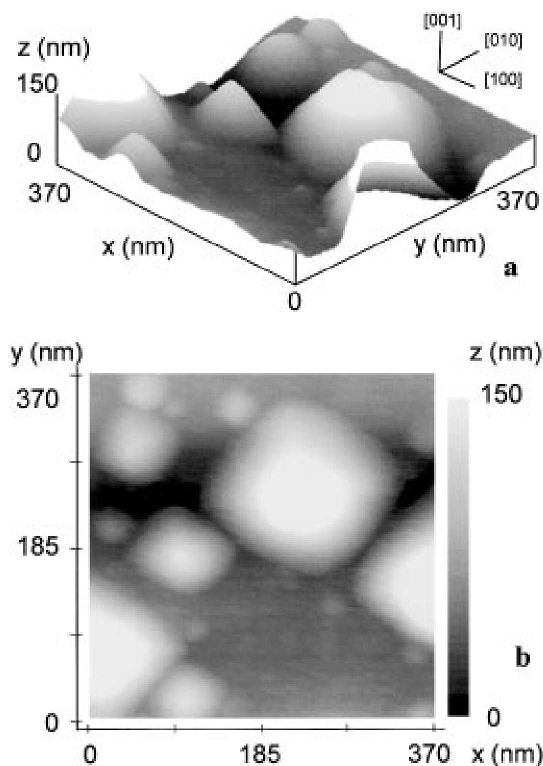

FIG. 2. Three-dimensional (a) and top view (b) images of the surface of the sample shown in Fig. 1 after 20 s additional etch in aqueous KOH solution.

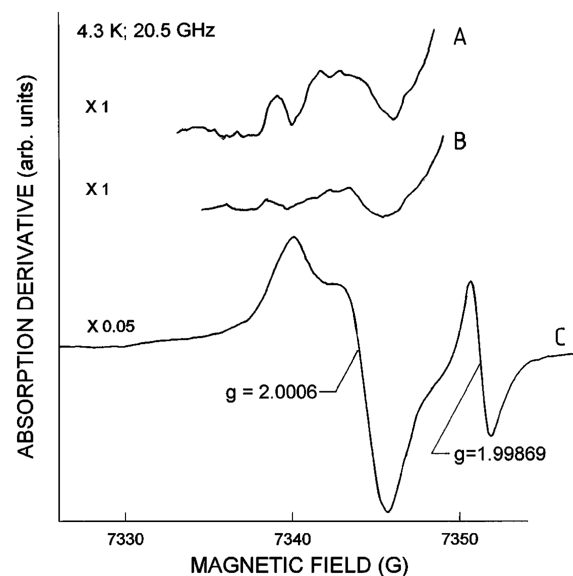

FIG. 3. K-band ESR spectra (4.3 K; applied microwave power ≤ 0.3 nW) after Ar ion bombardment of a single O^+ implanted $Si/SiO_2/Si$ structure with the oxide pyramids exposed (A, B) and a-SiO_2 thermally grown on (100) Si (C). Spectra A and B were taken with **B** perpendicular to the sample surface, and after 70° rotation around the [110] axis, respectively. The signal at $g = 1.998\,69$ stems from a Si:P reference sample.

increase accordingly. Another observation is that when the implantation is performed in multiple steps with intermittent high temperature annealing, no SiO_2 crystallites are observed. These observations suggest that the formation of the oxide crystallites occurs within a certain O-density window, i.e., neither too high nor too low an oxygen concentration in Si: they are absent in the bulk of the buried oxide, where the oxygen concentration is high after the implantation, but are observed in the less O-rich interface region. In the multiple implanted structures then the oxygen concentration during anneal appears too low overall to form observable oxide crystals. Despite the differences in the processing of the structures, the shape and the orientation of the oxide crystallites, when observed, is found to be identical. Importantly, this indicates that the nucleation and growth of the crystallites are controlled by the Si substrate crystallinity, i.e., it occurs epitaxially. The "anticrystal" shaping process may be excluded, because the observed pyramid bordering cannot be explained by, e.g., (111) planes of the Si substrate.

The shape of the oxide crystallites is close to that expected for coesite with (111) faces (monoclinic, $a = c = 7.17$ Å, $b = 12.38$ Å), the densified SiO_2 polymorph stable at high temperatures and pressures [20,21]. The $a/b = 0.579$ ratio of coesite may be compared with the experimental value of 0.57 ± 0.02. The b direction of the crystallites is along the normal to the substrate surface, while a is parallel to [100]. This is essentially the orientation found for the coesitelike oxygen precipitates in Si [10], also suggested to be formed at the Si/SiO_2 interface during oxidation [22]. This assignment is supported by TEM analysis, as exemplified in Fig. 4: The exposed pyramids provide additional diffraction incompatible with the Si substrate. Instead, they would refer to an additional crystalline phase of large elemental unit size, where the observed angle of 30° between these fringes and ⟨110⟩ silicon directions is consistent with diffraction of electrons on (111) coesite planes. It is very informative that we could trace the pyramidlike structures neither in the oxide thermally grown at 1000 °C or 1350 °C nor in the oxide produced by implanting such a high dose of oxygen that the entire top Si layer was consumed, followed by a 1350 °C postimplantation anneal (equilibrium oxide). So the presence of top silicon seems to be a prerequisite for crystallite formation. Apparently, the confinement of the oxide between two Si layers provides the pressure necessary to crystallize coesite during the postimplantation anneal.

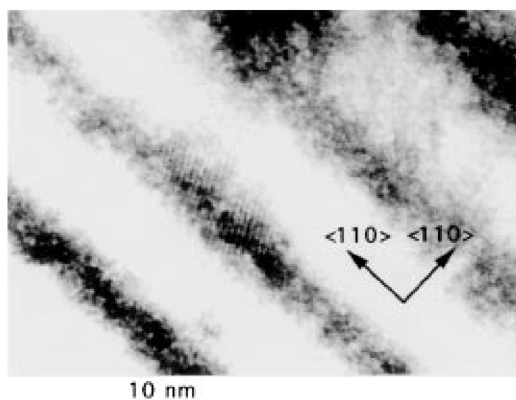

FIG. 4. Plain-view TEM image of a pyramid at the Si/oxide interface exposed by HF etching. The broad fringes originate from the Si substrate, while the narrow ones (in the center of the figure) refer to an additional crystalline phase.

The formation of the Si platelets, exposed by AFM images after HF etching of the oxide, is closely related to the presence of the oxide crystallites. The density and spatial location of the platelets closely matches the changes in the number and height of the oxide crystals when the processing is modified. A similar behavior is also observed for the photoactive electron traps in the oxide, associated with Si inclusions [11,12]. Thus the presence of different forms of excess silicon correlates with the formation of the oxide crystallites. The orientation of the Si platelets is in registry with the substrate and may be "heredited" via oxide crystals. One piece of evidence for this is inferred from the observation that due to cleavage of the Si platelet by the AFM tip at the HF-etched surface, the presence of the *underetched* oxide part is revealed during successive imaging. Thus a Si platelet is on top of a crystalline oxide basement. Such a feature can be explained if, during the buried oxide formation process, the oxide crystallites constitute a barrier for outdiffusion of excess silicon from the oxide to the substrate or top Si layer.

In conclusion, we have found that the oxide layers produced by the annealing of the silicon implanted with O^+ ions may contain a layer of crystallites, likely, coesite. The crystallites are oriented along Si substrate symmetry directions, suggesting their formation by three-dimensional epitaxial growth. The necessary condition for oxide crystallization is found confinement by a superficial Si layer.

[1] *The Physics of SiO_2 and Its Interfaces,* edited by S.T. Pantelides (Pergamon, New York, 1978).

[2] *The Physics of MOS Insulators,* edited by G. Lucovsky, S.T. Pantelides, and F.L. Galeener (Pergamon, New York, 1980).

[3] F.P. Fehlner, *Low Temperature Oxidation: The Role of Vitreous Oxides* (Wiley, New York, 1986).

[4] S.M. Sze, *Physics of Semiconductor Devices* (Wiley, New York, 1981), 2nd ed., p. 379.

[5] E.A. Irene, CRC Crit. Rev. Solid State Sci. **14**, 175 (1988).

[6] A. Ourmazd, D.W. Taylor, J.A. Rentschler, and J. Bevk, Phys. Rev. Lett. **59**, 213 (1987).

[7] K.H. Yang, H.F. Kappert, and G.H. Schwuttke, Phys. Status Solidi A **50**, 221 (1978).

[8] K. Wada, H. Nakanishi, H. Takaoka, and N. Inoue, J. Cryst. Growth **57**, 535 (1982).

[9] M. Itsumi, M. Tomita, and M. Yamawaki, Microelectronic Eng. **28**, 39 (1995).
[10] A. Bourret, J. Thibault-Dessaux, and D.N. Siedman, J. Appl. Phys. **55**, 825 (1984).
[11] V.V. Afanas'ev, G.A. Brown, H.L. Hughes, S.T. Liu, and A.G. Revesz, J. Electrochem. Soc. **143**, 347 (1996).
[12] V.V. Afanas'ev, A.G. Revesz, and H.L. Hughes, J. Electrochem. Soc. **143**, 695 (1996).
[13] A. Stesmans and K. Vanheusden, J. Appl. Phys. **76**, 1681 (1994).
[14] J. Margail, J. Stoemenos, C. Jaussaud, and M. Bruel, Appl. Phys. Lett. **54**, 526 (1989).
[15] S. Bagchi, J.D. Lee, S.J. Krause, and P. Roitman, in *Proceedings of 1995 IEEE International SOI Conference, Tucson* (IEEE, New York, 1995), p. 118.
[16] See, e.g., D.L. Griscom, Glass Sci. Technol. **4B**, 151 (1990).
[17] M. Antonini, P. Camagni, P.N. Gibson, and A. Manara, Radiat. Eff. **65**, 41 (1982).
[18] D.K. Stevens, W.J. Sturm, and R.H. Silsbee, J. Appl. Phys. **29**, 66 (1958).
[19] E. Rimini, *Ion Implantation: Basics to Device Fabrication* (Kluwer, Boston, 1995).
[20] R.W.G. Wyckhoff, *Crystal Structures* (Interscience, New York, 1974), 4th ed.
[21] S.T. Pantelides and W.A. Harrison, Phys. Rev. B **13**, 2667 (1976).
[22] B.J. Mrstik, A.G. Revesz, M. Ancona, and H.L. Hughes, J. Electrochem. Soc. **134**, 2020 (1987).